Degeneracy in carbon nanotubes under transverse magnetic δ-fields

Ş. Kuru*[1], J. Negro †[2], and S. Tristao‡[2]

[1]Department of Physics, Faculty of Science, Ankara University. 06100 Ankara, Turkey

[2]Departamento de Física Teórica, Atómica y Óptica, and IMUVA (Instituto de Matemáticas), Universidad de Valladolid. E-47011 Valladolid, Spain

Abstract

The aim of this paper is to study the degeneracy of the energy spectrum in a nanotube under a transverse magnetic field. The massless Dirac-Weyl equation has been used to describe the low energy states of this system. The particular case of a singular magnetic field approximated by Dirac delta distributions is considered. It is shown that, under general symmetry conditions, there is a degeneracy corresponding to periodic solutions with a null axial momentum $k_z = 0$. Besides, there may be present a kind of sporadic degeneracy for non-vanishing values of k_z, which are explicitly computed in the present example. The proof of these properties is obtained by means of the supersymmetric structure of the Dirac-Weyl Hamiltonian.

Keywords: Massless Dirac-Weyl equation, nanotube, spectrum degeneracy, supersymmetry.

1 Introduction

Single walled carbon nanotubes (CN) can be considered as a sheet of graphene rolled up to form a cylinder. Depending on the angle of the graphene lattice and the cylinder axis, the nanotube will inherit a metallic or semiconducting character [1–4].

The application of magnetic fields to a nanotube can have two kinds of effects. If the field is longitudinal (in the direction of the nanotube axis) it may interchange metallic and semiconducting behaviors by opening (or reducing) a gap in the band center. On the other

*email: kuru@science.ankara.edu.tr

†email: jnegro@fta.uva.es

‡email: rucksandaokan@yahoo.es

hand, transverse magnetic fields in general will increase the metallic character by reducing the initial gap [4–9].

The description of the low energy states of nanotubes, near each of the two Fermi points, can be done in the continuous limit of a tight binding model by means of the massless Dirac-Weyl equation, provided the circumference length $L = 2\pi\rho_0$ is much larger than the C-C distance a [4]. In the presence of a magnetic field of intensity B, the interaction can be described by the minimal coupling rule in the Dirac equation if $\frac{\hbar c}{qB}$ is much larger than $a\rho_0$, in order to avoid lattice effects [7]. The different types of nanotubes can be taken into account in the continuum limit by means of certain quasi-periodic conditions [4].

In this paper we will make use of this picture of low energy states to study the interaction of a nanotube with a singular transverse magnetic field that can be approximated by a Dirac delta. We want to address the question of the degeneracy of the energy spectrum. There are many references dealing with the electronic properties of nanotubes in transverse magnetic fields, but in general the problem of degeneracy has not been fully explained. For instance, in [7] it is given a discussion on this point in order to show a quantum Hall effect in nanotubes, but this is done on a rather qualitative ground. We want to deduce the degeneracy properties just from the symmetries of the periodic Dirac-Weyl equation. The natural way to get a satisfactory answer to this problem is by making use of supersymmetry arguments. Each component of the Dirac spinor satisfies an effective Schrödinger equation of a supersymmetric couple [10]. The connection of the symmetry properties of these two effective equations will lead us to a global symmetry explaining the degeneracy.

In this work we have chosen a Dirac delta singular magnetic field to illustrate this problem. There are several reasons for this choice: (i) Although not realistic, this is a very simple case where all the possible types of degeneracy can be explained in a clear way. (ii) This potential is quite different from that of a constant background magnetic field, which is better known in the literature [4,7,9], so that it will constitute a good test to check some known properties. In any case, the same symmetry concepts can also be applied to any other magnetic field in order to find its degeneracy. The paper is organized as follows. Section II introduces the notation to describe the interaction of quasi-particles in nanotubes under a generic transverse magnetic field. In particular, the supersymmetric form of the Dirac-Weyl Hamiltonian is shown as well as the two effective partner Schrödinger Hamiltonians [10]. Next, in Section III this formalism is applied to a transverse singular Dirac delta field. The spectrum and the form of the current in the axis direction will be obtained. The degeneracy is studied in Section IV. There are two types of degeneracy: (i) the corresponding to periodic eigenfunctions for quasi-particles with null axial momentum, and (ii) a kind of 'sporadic' degeneracy that can be present in some special cases of non-vanishing axial momentum. The last section is devoted to some remarks and conclusions.

2 Nanotube in external magnetic fields

We will start with the general formalism to describe the quasi-particles of a nanotube in a magnetic field at low energies. In principle, the magnetic field at each point of the nanotube surface can be decomposed into transverse $\mathbf{B}_\perp$ (perpendicular to the surface) and parallel $\mathbf{B}_\parallel$ (tangent to the surface) components. As the Lorentz force produced by the magnetic field is perpendicular to the motion of the charged particles, only the perpendicular component is effective in this situation. The other components, specially the longitudinal component along the nanotube axis, may have another kind of influence that will not be considered here [5, 6, 9, 11].

Let us take cylindrical coordinates (ρ, ϕ, z), where the z-axis is along the nanotube axis. Since the magnetic field $\mathbf{B}$ produced by the vector potential $\mathbf{A} = A_\rho \mathbf{n}_\rho + A_\phi \mathbf{n}_\phi + A_z \mathbf{n}_z$ is

$$\mathbf{B} = \nabla \times \mathbf{A} = \left(\frac{1}{\rho}\partial_\phi A_z - \partial_z A_\phi\right)\mathbf{n}_\rho + \left(\partial_z A_\rho - \partial_\rho A_z\right)\mathbf{n}_\phi + \left(\partial_\rho A_\phi - \partial_\phi A_\rho + \frac{A_\phi}{\rho}\right)\mathbf{n}_z \quad (1)$$

then, the effective magnetic field perpendicular to the nanotube surface at $\rho = \rho_0$ will be given by

$$\mathbf{B}_\perp = \left(\frac{1}{\rho_0}\partial_\phi A_z - \partial_z A_\phi\right)\mathbf{n}_\rho \,. \quad (2)$$

This effective field can be described by a vector potential tangent to the surface of the nanotube,

$$\mathbf{A} = A_\phi(\phi, z)\mathbf{n}_\phi + A_z(\phi, z)\mathbf{n}_z \,. \quad (3)$$

In the low energy limit, a quasi-particle interacting with the effective magnetic field $\mathbf{B}_\perp$ is described by the massless Dirac-Weyl equation [4, 11] via the minimal coupling with the vector potential (3),

$$\left[-\sigma_2\left(i\partial_z + \frac{q}{c\,\hbar}A_z\right) + \sigma_1\left(\frac{i}{\rho_0}\partial_\phi + \frac{q}{c\,\hbar}A_\phi\right)\right]\hat{\Psi}(z,\phi) = \epsilon\,\hat{\Psi}(z,\phi), \quad (4)$$

where $\epsilon = \frac{E}{v_F\hbar}$. Now, the wave functions $\hat{\Psi}(z,\phi)$ that we are looking for are subject to the boundary condition

$$\hat{\Psi}(z, 2\pi) = e^{i\,2\pi\delta}\hat{\Psi}(z, 0), \quad (5)$$

where $-1/2 < \delta \leq 1/2$ is the phase shift after a period of the angular variable. Since the values δ and $-\delta$ are related by a complex conjugation in (5), hereafter we will restrict to positive values $0 \leq \delta \leq 1/2$. The concrete value of δ to be considered will depend on the properties of the nanotube: it is related to the particular way a piece of planar graphene is rolled in order to construct the nanotube or to other longitudinal magnetic fields [4].

Here, we will deal with the case where $\mathbf{B}_\perp$ does not depend on z but it is a function of ϕ. This situation can be described by the potential

$$(A_\phi = 0, A_z = A_z(\phi)) \quad \Longrightarrow \quad \mathbf{B}_\perp(\phi) = \frac{1}{\rho_0}\partial_\phi A_z(\phi)\,\mathbf{n}_\rho \,. \quad (6)$$

Due to the symmetry under translation in the z-direction, the stationary equation (4) can be separated by taking the wave function in the form

$$\hat{\Psi}(z,\phi) = e^{ik_z z}\Psi(\phi), \qquad \Psi(\phi) = \begin{pmatrix} \psi^1(\phi) \\ \psi^2(\phi) \end{pmatrix}. \tag{7}$$

Thus, we get a one dimensional stationary equation depending on the constant momentum $p_z = \hbar k_z$ of the particle in the z-direction,

$$\left[i\sigma_1\partial_\phi + \left(\rho_0 k_z - \frac{\rho_0 q}{c\hbar}A_z(\phi)\right)\sigma_2\right]\Psi(\phi) = \rho_0\,\epsilon\,\Psi(\phi), \tag{8}$$

together with the boundary condition

$$\Psi(\phi + 2\pi) = e^{i2\pi\delta}\Psi(\phi), \qquad 0 \le \delta \le 1/2\,. \tag{9}$$

Equation (8) represents two coupled, first-order differential equations for the spin-up and down components $\psi^1(\phi)$ and $\psi^2(\phi)$, respectively. Let us introduce the operators

$$\mathcal{A}^\dagger \;=\; \partial_\phi + W(\phi), \qquad \mathcal{A} = -\partial_\phi + W(\phi), \tag{10}$$

where

$$W(\phi) = -\rho_0 k_z + \frac{\rho_0 q}{c\hbar}A_z(\phi). \tag{11}$$

In terms of these operators, equation (8) can be cast in a more appealing form:

$$H\,\Psi(\phi) = \begin{pmatrix} 0 & i\,\mathcal{A}^\dagger \\ -i\,\mathcal{A} & 0 \end{pmatrix}\Psi(\phi) = \tilde{\epsilon}\,\Psi(\phi), \qquad \tilde{\epsilon} = \rho_0\epsilon\,. \tag{12}$$

This equation can be decoupled by applying H to the left, so that we obtain a diagonal second order Hamiltonian H^2,

$$H^2\,\Psi(\phi) \equiv \begin{pmatrix} H_1 & 0 \\ 0 & H_2 \end{pmatrix}\Psi(\phi) = \begin{pmatrix} \mathcal{A}^\dagger\mathcal{A} & 0 \\ 0 & \mathcal{A}\mathcal{A}^\dagger \end{pmatrix}\Psi(\phi) = \tilde{\epsilon}^2\,\Psi(\phi) \tag{13}$$

where

$$H_1 \equiv \mathcal{A}^\dagger\mathcal{A} = -\partial_\phi^2 + W^2(\phi) + \frac{dW(\phi)}{d\phi}, \quad H_2 \equiv \mathcal{A}\mathcal{A}^\dagger = -\partial_\phi^2 + W^2(\phi) - \frac{dW(\phi)}{d\phi}. \tag{14}$$

Therefore, the upper (ψ^1) and lower (ψ^2) components of $\Psi(\phi)$ must be eigenfunctions of the effective Schrödinger Hamiltonians H_1 and H_2, respectively, with the same effective energy $\tilde{\epsilon} = \rho_0^2\epsilon^2$. If the eigenvalue is nonzero, according to (12) these components are related by means of the operators (10),

$$\psi^1 = \frac{i}{\tilde{\epsilon}}\,\mathcal{A}^\dagger\psi^2, \qquad \psi^2 = -\frac{i}{\tilde{\epsilon}}\,\mathcal{A}\psi^1. \tag{15}$$

The zero modes $\Psi_0 = (\psi_0^1, \psi_0^2)^T$ of the Hamiltonian H can be found by solving the following equations

$$\mathcal{A}^\dagger \psi_0^2 = 0, \qquad \mathcal{A}\psi_0^1 = 0. \tag{16}$$

Only when the solutions to these 1st order equations satisfy the boundary conditions, they give rise, respectively, to the zero energy solutions

$$\Psi_0^\uparrow = \begin{pmatrix} \psi_0^1 \\ 0 \end{pmatrix}, \qquad \Psi_0^\downarrow = \begin{pmatrix} 0 \\ \psi_0^2 \end{pmatrix}. \tag{17}$$

In the frame of supersymmetric quantum mechanics, we say that the Hamiltonians H_1 and H_2 are supersymmetric partners, the operators $\mathcal{A}, \mathcal{A}^\dagger$ are intertwining operators and the function $W(\phi)$ is the superpotential. The spectral problem for the matrix Hamiltonian (12) is equivalent to that of the common spectrum of the scalar Hamiltonians H_1 and H_2 given in (14). The effective potentials of these scalar Hamiltonians are given, according to (14), by

$$V_1(\phi) = W^2(\phi) + \frac{dW(\phi)}{d\phi}, \qquad V_2(\phi) = W^2(\phi) - \frac{dW(\phi)}{d\phi}. \tag{18}$$

These scalar potentials will help us to interpret the behavior of the components $\psi^1(\phi)$ and $\psi^2(\phi)$ in the original matrix equation (12). The boundary conditions on the eigenfunctions $\psi^{1,2}(\phi)$ of the scalar Hamiltonians are the same as in (9),

$$\psi^{1,2}(\phi + 2\pi) = e^{i2\pi\delta}\psi^{1,2}(\phi), \qquad 0 \le \delta \le 1/2. \tag{19}$$

3 Transverse magnetic δ-fields

We will consider a magnetic field that enters in the nanotube near the point $\phi = \pi/2$ with a singular intensity given in terms of the Dirac delta distribution, and leaves the nanotube at the opposite point $\phi = -\pi/2$ with the same intensity. This field is described by the magnetic potential

$$A_z(\phi) = A_0\,[H(\phi + \pi/2) + H(-\phi + \pi/2) - 3/2], \qquad -\pi \le \phi \le \pi, \tag{20}$$

where $H(\phi)$ is the Heaviside function (see Fig. 1). Then, according to (6), the magnetic field has the expression

$$\mathbf{B}_\perp = \frac{A_0}{\rho_0}\big(\delta(\phi + \pi/2) - \delta(\phi - \pi/2)\big)\mathbf{n}_\rho \equiv B(\phi)\mathbf{n}_\rho. \tag{21}$$

There are two important aspects of the potential function to be remarked.

(i) As ϕ is an angular variable, the potential $A_z(\phi)$ in (20) can be extended to a periodic real function with period $T = 2\pi$.

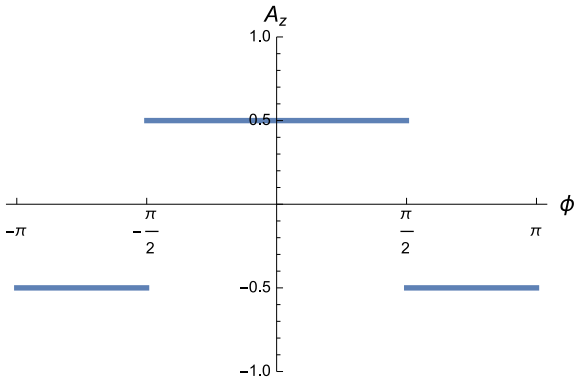

Figure 1: The potential $A_z(\phi)$ given in (20) for $A_0 = 1$.

(ii) The integral of $A_z(\phi)$ along a period vanishes: $\int_0^{2\pi} A_z(\phi)\, d\phi = 0$.

The next step is replacing this magnetic potential in the eigenvalue equation (26) for the effective Hamiltonians H_1 and H_2 with effective potentials (18). It will be useful to introduce the following constants

$$\alpha = \rho_0\, k_z, \qquad \beta = \frac{\rho_0\, q}{c\hbar} \tag{22}$$

so that

$$W(\phi) = -\alpha + \beta\, A_z(\phi)\,. \tag{23}$$

Notice that, once fixed the radius of the nanotube, the parameter α is proportional to the momentum k_z in the z–direction. Then, the explicit form of the effective potentials is (see Fig. 2)

$$V_1(\phi) = \alpha^2 + \frac{\beta^2 A_0^2}{4} - 2\beta\alpha A_z(\phi) + \beta\rho_0 B(\phi) = V_0(\phi) + \beta\rho_0 B(\phi)\,, \tag{24}$$

$$V_2(\phi) = \alpha^2 + \frac{\beta^2 A_0^2}{4} - 2\beta\alpha A_z(\phi) - \beta\rho_0 B(\phi) = V_0(\phi) - \beta\rho_0 B(\phi)\,. \tag{25}$$

Thus, the effective potentials include two terms:

(i) A common term, $V_0(\phi)$, with a part proportional to the magnetic potential, $-2\beta\alpha A_z(\phi)$, plus a constant $M \equiv \alpha^2 + \frac{\beta^2 A_0^2}{4}$ (depending on k_z and ρ_0).

(ii) A second term proportional to the magnetic field intensity: $\pm\beta\rho_0 B(\phi)$ (with plus sign for V_1 and minus sign for V_2). This term contains the Dirac delta singularities.

In order to solve the spectral problem, we can choose just one of the Hamiltonians H_1 or H_2, since the solutions for the other one are found through the relations (15) or (16).

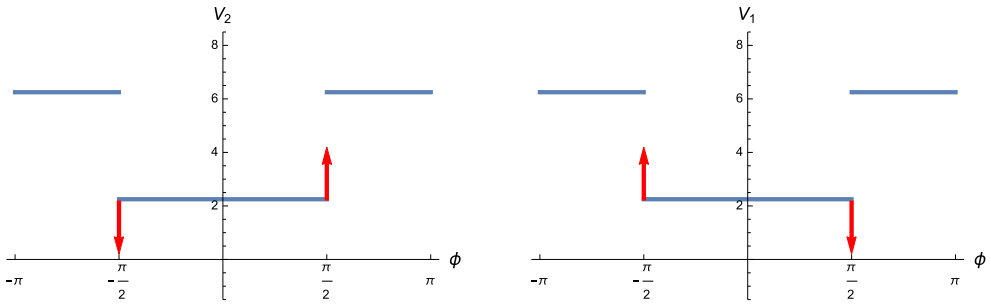

Figure 2: Effective potentials $V_2(\phi)$ (left) and $V_1(\phi)$ (right) for $\alpha = 2$, $\beta = 1$, $A_0 = 1$. The δ singularities are represented by arrows at the discontinuity points.

Henceforth, we will take H_2 and write down its eigenvalue equation:

$$H_2\,\psi(\phi) = \tilde{\epsilon}^2\,\psi(\phi), \qquad \psi(\phi) \equiv \psi^2(\phi)\,. \tag{26}$$

This equation can be divided in the three regions of the interval $[-\pi, \pi]$ where the finite potential V_0 takes constant values (see Fig. 2):

$$V_0(\phi) = \begin{cases} M+N, & -\pi < \phi < -\pi/2 \qquad (I) \\ M-N, & -\pi/2 < \phi < \pi/2 \qquad (II) \\ M+N, & \pi/2 < \phi < \pi \qquad (III) \end{cases} \qquad M = \alpha^2 + \frac{\beta^2 A_0^2}{4}, \quad N = \beta\alpha A_0\,. \tag{27}$$

If $\alpha \to 0$, then $N \to 0$, so that in this case $V_0(\phi)$ will remain constant and the only significant contribution to the effective potential will come from the singular magnetic field.

The solutions corresponding to a fixed effective energy $\tilde{\epsilon}^2$ consist of the free Schrödinger solutions in the three regions subject to appropriate matching and periodic conditions,

$$\begin{aligned} &\left[\tfrac{d^2}{d\phi^2} - {\kappa_1}^2\right]\psi_I(\phi) = 0, && -\pi < \phi < -\pi/2, && {\kappa_1}^2 = (M+N) - \tilde{\epsilon}^2 \\ &\left[\tfrac{d^2}{d\phi^2} - {\kappa_2}^2\right]\psi_{II}(\phi) = 0, && -\pi/2 < \phi < \pi/2, && {\kappa_2}^2 = (M-N) - \tilde{\epsilon}^2 \\ &\left[\tfrac{d^2}{d\phi^2} - {\kappa_1}^2\right]\psi_{III}(\phi) = 0, && \pi/2 < \phi < \pi, && {\kappa_1}^2 = (M+N) - \tilde{\epsilon}^2\,. \end{aligned} \tag{28}$$

The matching conditions at $\phi = \pm\pi/2$ are determined by the Dirac delta singularities of the magnetic term of the potential at these points:

$$\begin{aligned} &\psi_I(-\pi/2) = \psi_{II}(-\pi/2)\,, && \psi_{II}(\pi/2) = \psi_{III}(\pi/2)\,, \\ &\psi_I'(-\pi/2) = \psi_{II}'(-\pi/2) + \beta A_0 \psi_I(-\pi/2)\,, && \psi_{II}'(\pi/2) = \psi_{III}'(\pi/2) - \beta A_0 \psi_I(\pi/2)\,. \end{aligned} \tag{29}$$

Besides, there must be added the periodicity conditions at $\phi = \pm\pi$:

$$\psi_{III}(\pi) = e^{i\,2\pi\delta}\psi_I(-\pi), \qquad \psi'_{III}(\pi) = e^{i\,2\pi\delta}\psi'_I(-\pi)\,. \tag{30}$$

When solving this problem, one must have in mind that there are three types of values the effective energy $\tilde{\epsilon}^2$ can take (here we are assuming $\alpha > 0$):

$$(i)\quad \tilde{\epsilon}^2 > M+N, \qquad (ii)\quad M+N > \tilde{\epsilon}^2 > M-N, \qquad (iii)\quad M-N > \tilde{\epsilon}^2\,. \tag{31}$$

3.1 Periodic solutions

If we choose $\delta = 0$, we get the periodic solutions. This situation corresponds to the case where the lattice consists in hexagons matching well around the nanotube [4]. In this case, the longitudinal field is also vanishing. We have to solve the spectrum in the three different ranges of the effective energy mentioned above. This is given by the following simple formulas:

$$\begin{aligned}
&\tilde{\epsilon}^2 > M+N, \quad \kappa_j = ik_j, \quad j=1,2\\
&k_1(2k_1k_2(-1+\cos(k_1\pi)\cos(k_2\pi)) + (A_0^2\beta^2 + k_1^2 + k_2^2)\sin(k_1\pi)\sin(k_2\pi)) = 0\,,\\
&M+N > \tilde{\epsilon}^2 > M-N, \quad \kappa_1 = k_1, \quad \kappa_2 = i\,k_2\\
&k_1(2k_1k_2(-1+\cosh(k_1\pi)\cos(k_2\pi)) - (A_0^2\beta^2 - k_1^2 + k_2^2)\sinh(k_1\pi)\sin(k_2\pi)) = 0\,,\\
&M-N > \tilde{\epsilon}^2, \quad \kappa_j = k_j, \quad j=1,2\\
&k_1(2k_1k_2(-1+\cosh(k_1\pi)\cosh(k_2\pi)) + (-A_0^2\beta^2 + k_1^2 + k_2^2)\sinh(k_1\pi)\sinh(k_2\pi)) = 0\,.
\end{aligned} \tag{32}$$

The plot of the resulting spectrum as a function of the 'momentum' α is displayed in Fig. 3 for three values of the field intensity, $A_0 = 1, 5, 10$. This is similar to Fig. 2 of Ref. [7] for constant magnetic fields. The most important feature, regarding the degeneracy, is that all the energy levels, for any magnetic field intensity, are degenerate at $k_z = 0$ ($\alpha = 0$). Notice that for $k_z = 0$ the two effective potentials (24) and (25) are simpler:

$$V_1(\phi) = \frac{\beta^2 A_0^2}{4} + \beta\rho_0 B(\phi), \qquad V_2(\phi) = \frac{\beta^2 A_0^2}{4} - \beta\rho_0 B(\phi)\,. \tag{33}$$

This means that both, $V_1(\phi)$ and $V_2(\phi)$, are symmetric with respect to the reflection around the singular points $\phi_n = -\frac{\pi}{2} + n\,\pi$. We will show in the next section that, indeed in this situation the energy levels of the periodic solutions must be degenerate.

When $|k_z| > 0$ this symmetry is broken, the degeneration is lifted and all the levels become non-degenerated. However, for greater values of $|k_z|$ there can appear 'sporadic' degeneracies at certain values of $|k_z|$ as can be appreciated in Fig. 3. The reason is that in this situation there remains a certain symmetry: observe that in Fig. 2 the effective

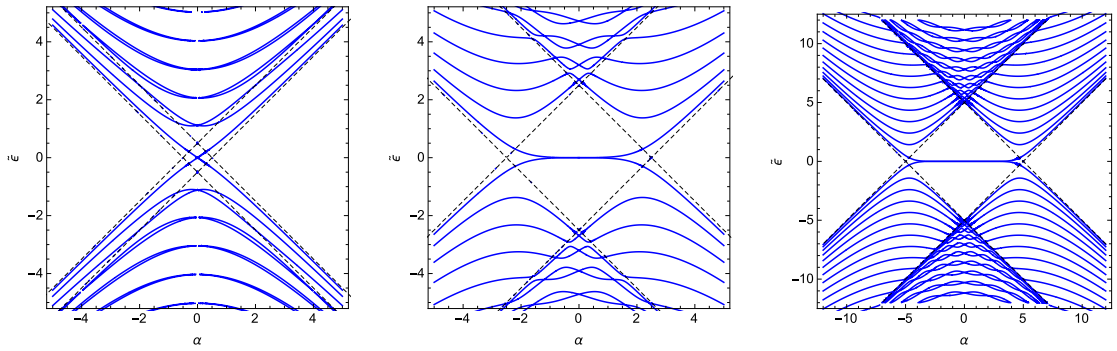

Figure 3: Spectrum of the energies $\tilde{\epsilon} = \frac{\rho_0}{v_F \hbar} E$ of periodic solutions as functions of $\alpha = \rho_0 k_z$ for different intensities of the magnetic field (21): $A_0 = 1$ (left), $A_0 = 5$ (center), $A_0 = 10$ (right) in units of $\frac{\rho_0 q}{c\hbar}$ (this is equivalent to set $\beta = 1$ in (27)). The dotted lines in black correspond to the values $M + N$, $M - N$ of the finite part (27) of the effective potentials V_1, V_2.

potentials V_1 and V_2 are related by means of a reflection, $V_1(\phi) = V_2(-\phi)$. As we will see later, this property will be the origin of sporadic degeneracies in this case.

In Fig. 3 it is also shown the effect of increasing the intensity of the magnetic field on the spectrum. The gap of the central energy levels is reduced even for larger values of k_z as the magnetic field is bigger. Thus, the metallic behavior is strengthened by the intense magnetic fields [4, 7].

Of course, we should also mention the trivial symmetry of the spectrum with respect to the sign of k_z.

Once we know the spectrum and solutions for periodic functions, we can compute the density current j_z in the direction of the nanotube axis. According to the notation of (7) this is given by

$$j_z = \hat{\Psi}(z,\phi)^\dagger \sigma_2 \hat{\Psi}(z,\phi) = \Psi(\phi)^\dagger \sigma_2 \Psi(\phi)\,. \tag{34}$$

The components ψ^1 and ψ^2 of Ψ are related by (15), $\psi^1 = \frac{i}{\tilde{\epsilon}} \mathcal{A}^+ \psi^2$, as far as $\tilde{\epsilon} \neq 0$ (in case $\tilde{\epsilon} = 0$ the density current will vanish). The component ψ^2 will be a solution of the effective Hamiltonian H_2 as written in (26) and in the periodic case it can always be chosen real. Replacing these components in (34) we have

$$j_z(\phi) = -\frac{2}{\tilde{\epsilon}}\, \psi^2 \mathcal{A}^+ \psi^2\,. \tag{35}$$

Now, we are in conditions to compute the density current for any periodic solution of the above spectrum. In Figs. 4–7 it is shown the wavefunctions and their corresponding currents of periodic solutions for $\alpha = \pm 3$, $A_0 = 5$ at four different energies.

Due to the relation of the total current with the dispersion relation [7], when $k_z = 0$ we will have

$$\int_0^{2\pi} j_z(\phi)\, d\phi = 0\,. \tag{36}$$

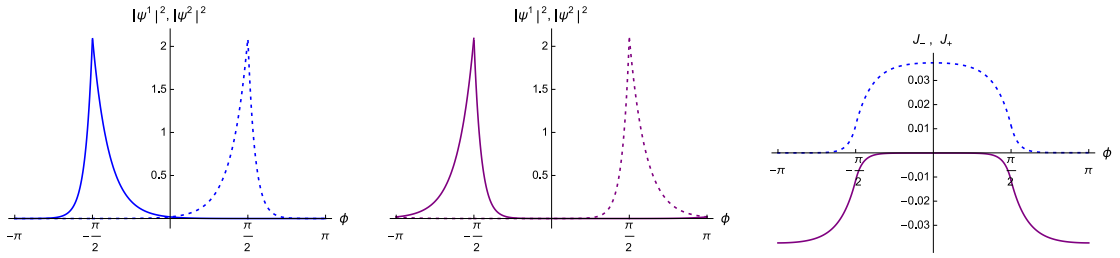

Figure 4: Squared wave-functions corresponding to positive α at the left in blue, and to negative α at the center in purple. The corresponding current densities are shown at the right (for positive α in dashing blue, for α negative in continuous purple line). Values: $\alpha = \pm 3, \beta = 1, A_0 = 5, \tilde{\epsilon} = 0.018$ ($\tilde{\epsilon}^2 < M - |N|$).

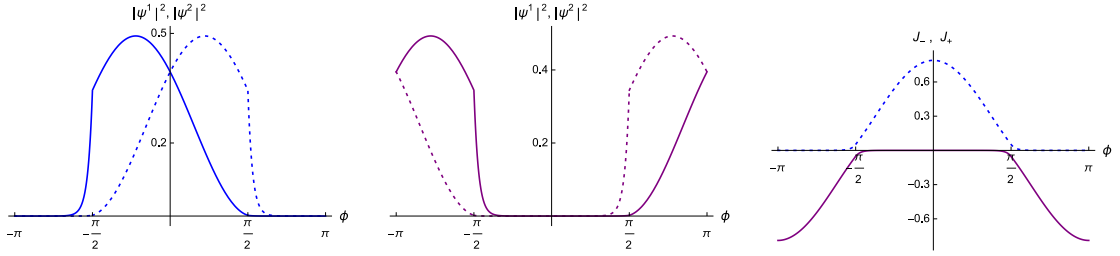

Figure 5: The same as Fig. 4 but for higher energy: $\tilde{\epsilon} = 0.831$ ($M - |N| < \tilde{\epsilon}^2 < M + |N|$).

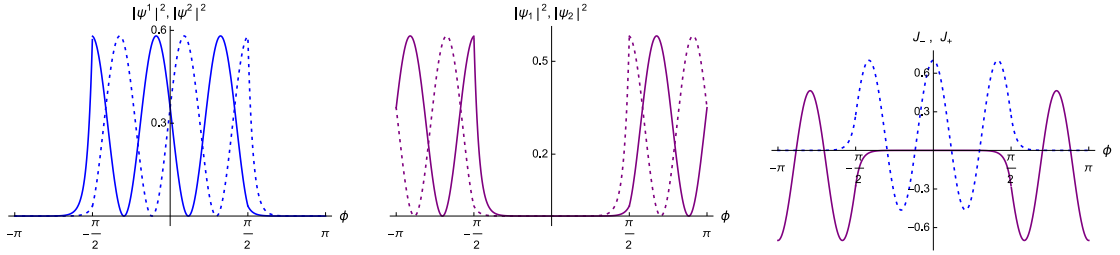

Figure 6: The same as Fig. 4 and Fig. 5 for energy $\tilde{\epsilon} = 2.464$ ($M - |N| < \tilde{\epsilon}^2 < M + |N|$).

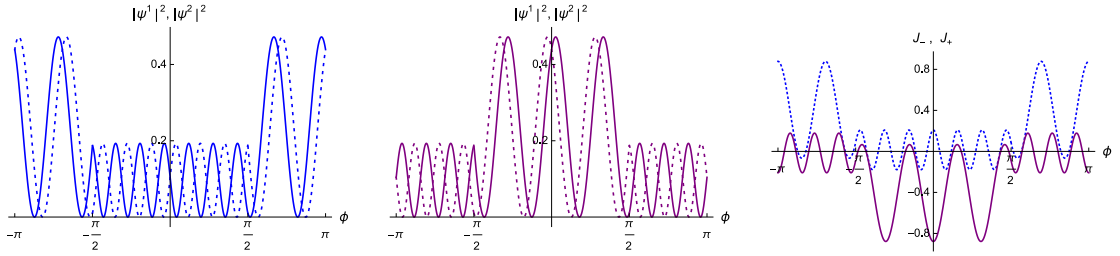

Figure 7: The same as Figs. 4-6 for energy $\tilde{\epsilon} = 6.396$ ($M + |N| < \tilde{\epsilon}^2$).

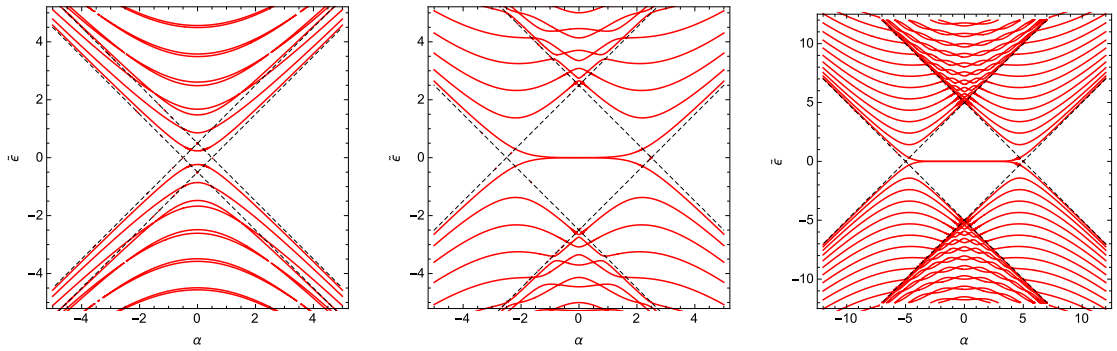

Figure 8: Spectrum of the energies $\tilde{\epsilon}$ of anti-periodic solutions as functions of $\alpha = \rho_0 k_z$ for different values of the magnetic field: $A_0 = 1$ (left), $A_0 = 5$ (center), $A_0 = 10$ (right) and $\beta = 1$. The dotted curves in black correspond to the values $M + N$ and $M - N$ of the finite part (27) of the effective potentials V_1, V_2.

However, for $k_z > 0$ ($k_z < 0$) the net current is positive (negative), and it becomes larger as we increase k_z. This phenomenon describes a non null flux of charged particles corresponding to axial linear momentum k_z. It should be remarked that while the positive current for positive values $k_z > 0$ is restricted to one of the subintervals $|\phi| < \pi/2$ or $\pi > |\phi| > \pi/2$, the current for negative values $k_z < 0$ will be present just in the other subinterval. Thus, it is like having a highway with two separate lanes, each one for a different sign of k_z carrier.

3.2 Anti-periodic solutions

The anti-periodic solutions are obtained for the value $\delta = 1/2$. The equations for the matching and anti-periodic conditions are similar to the previous case (32). A plot of the resulting spectrum is given in Fig. 8 for three different values of the magnetic field. It is shown that, for low field intensities ($A_0 \approx 1$), at $k_z = 0$ the spectrum is not degenerated (contrary to the periodic case). An example of anti-periodic solution at $\alpha = 0$ is represented in Fig. 9. As the field intensity becomes higher the lowest energy level becomes degenerated, thus enhancing the metallic character (see in Fig. 8 the plots in the center and to the right). We can also observe that when $|k_z|$ is increasing some 'sporadic' degeneration can appear for any field intensity; this is similar to the sporadic degeneracy of periodic solutions, whose explanation will be given in the next section.

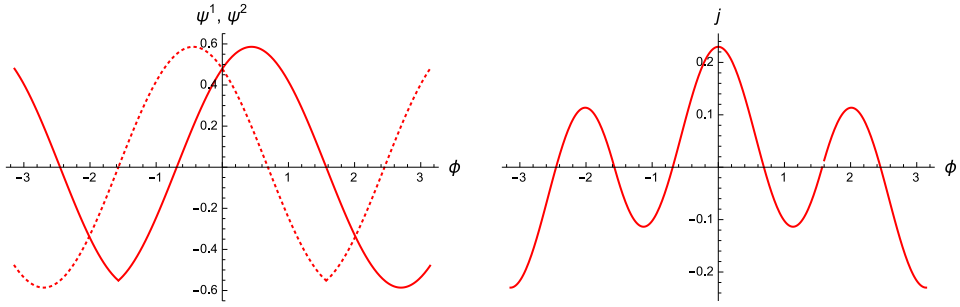

Figure 9: Components of the anti-periodic eigenfunction $\Psi = (i\,\psi^1, \psi^2)^T$ (left) at $\alpha = 0$, for an effective energy $\tilde{\epsilon} = \sqrt{2.18}$ with $\beta = 1, A_0 = 1$ (left). The (real part of) first component ψ^1 is represented by a dashing line while the second one ψ^2 is in continuous curve, the density current $j(\phi)$ is on the right.

4 Degeneracy of the spectrum

4.1 Degeneracy of the spectrum of periodic solutions at $k_z = 0$

As remarked above, when $k_z = 0$ the spectrum of periodic solutions is degenerated. In this section we will explain the reason for the degeneracy as well as why this degeneracy does not affect to other solutions (for instance, to anti-periodic solutions). The proof of this property lies in the supersymmetric character of the effective Hamiltonians given by (14) in terms of $W(\phi)$. According to (11) if $k_z = 0$ the superpotential $W(\phi)$ coincides, up to a multiplicative constant, just with the magnetic potential A_z (20),

$$W(\phi) = \beta\, A_z(\phi)\,. \tag{37}$$

In this situation, let us enumerate the symmetry properties of $W(\phi)$ which are immediate from Fig. 1 (the angular variable ϕ is assumed to range over $\mathbb{R}$):

(i) Periodicity with period $T = 2\pi$:

$$W(\phi) = W(\phi + 2\pi)\,. \tag{38}$$

(ii) Anti-symmetry with respect to reflections around the points $\phi_n = \frac{\pi}{2} + n\,\pi$, $n \in \mathbb{Z}$:

$$W(\phi + \phi_n) = -W(-\phi + \phi_n)\,. \tag{39}$$

(iii) Anti-periodicity with anti-period $A = \pi$:

$$W(\phi) = -W(\phi + \pi)\,. \tag{40}$$

This list of properties for the superpotential leads to corresponding properties of the associated potentials V_1, V_2:

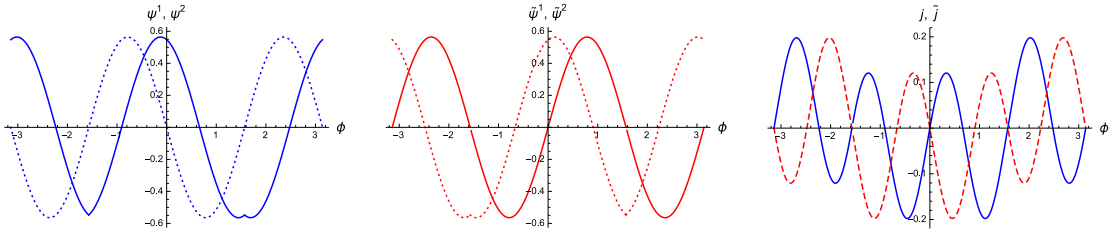

Figure 10: Components of two independent periodic eigenfunctions $\Psi = (i\,\psi^1, \psi^2)^T$ (left) and $\tilde{\Psi} = (i\,\tilde{\psi}^1, \tilde{\psi}^2)^T$ (center) for a degenerated effective energy $\tilde{\epsilon} = \sqrt{4.25}$ at $\alpha = 0$ with $\beta = 1, A_0 = 1$. The (real part of) the first components ψ^1 and $\tilde{\psi}^1$ are represented by dashing lines while the second ones ψ^2 and $\tilde{\psi}^2$ are in continuous lines. Density currents $j(\phi), \tilde{j}(\phi)$ for the solutions Ψ (continuous) and $\tilde{\Psi}$ (dashing) are represented to the right.

(i′) Both potentials V_1, V_2 are periodic with period $T = 2\pi$:

$$V_i(\phi) = V_i(\phi + 2\pi), \qquad i = 1, 2\,. \tag{41}$$

(ii′) Both potentials V_1, V_2 are symmetric with respect to reflections around the points $\phi_n = \frac{\pi}{2} + n\,\pi$, $n \in \mathbb{Z}$:

$$V_i(\phi + \phi_n) = V_i(-\phi + \phi_n), \qquad i = 1, 2\,. \tag{42}$$

(iii′) The partner potentials V_1, V_2 are π-displaced from each other:

$$V_1(\phi) = V_2(\phi + \pi)\,. \tag{43}$$

To prove the properties (i′)-(iii′) from (i)-(iii) it is enough to make use of the defining formulas (18) of V_1, V_2 in terms of $W(\phi)$.

Now, let us concentrate in the periodic solutions of Hamiltonian H_2 with potential V_2 characterized by the above properties. Since V_2 is ϕ_n–symmetric, which is compatible with the 2π–periodicity, this implies that we can classify each periodic solution in ϕ_n–symmetric or ϕ_n–anti-symmetric. This means, for example, that if ψ is both 2π-periodic and ϕ_0-symmetric, then necessarily it should also be ϕ_n–symmetric for all $n \in \mathbb{Z}$. Or if ψ is both 2π–periodic and ϕ_0–anti-symmetric, then necessarily it should also be ϕ_n–anti-symmetric $\forall n \in \mathbb{Z}$. As an example, the periodic solution ψ^2 shown in Fig. 10 (left, continuous curve) is ϕ_n–symmetric while $\tilde{\psi}^2$ is ϕ_n–antisymmetric (center, continuous curve).

Let ψ^2 be a 2π-periodic eigenfunction of H_2, such that for example, it is also ϕ_n-symmetric. Then, according to (15), the function $\psi^1 = \frac{i}{\epsilon}\mathcal{A}^\dagger\psi^2$ will be a solution of H_1. Since $\mathcal{A}^\dagger(\phi)$ is a ϕ_n–anti-symmetric operator, the resulting function ψ^1 will be ϕ_n–anti-symmetric. Therefore, the symmetric/antisymmetric character of ψ^1 is opposite to that of ψ^2. For example, in Fig. 10 (left) it is seen that the periodic solution ψ^1 (dashing) is ϕ_n–anti-symmetric while ψ^2 is ϕ_n-symmetric (continuous).

On the other hand, from property (iii′) (43), as $H_1(\phi+\pi) = H_2(\phi)$, we have that $\tilde{\psi}^2(\phi) = \psi^1(\phi+\pi)$ is an eigenfunction of $H_2(\phi)$. Therefore, we have the initial eigenfunction $\psi^2(\phi)$ and the new eigenfunction $\tilde{\psi}^2(\phi)$ of H_2. As each of these eigenfunctions has different character to the other (one is ϕ_n-symmetric while the other is ϕ_n–anti-symmetric), they must be independent, and therefore the eigenvalue is degenerate. As an illustration, the eigenfunctions ψ^2 and $\tilde{\psi}^2$, shown in Fig. 10, correspond to the same eigenvalue and they have different ϕ_n–symmetric/anti-symmetric character.

Now, let us consider briefly the case of anti-periodic eigenfunctions of H_2. In this case the function ψ^2 satisfies $\psi(\phi+2\pi) = -\psi(\phi)$. If ψ^2 is ϕ_0-symmetric, due to the anti-periodicity it will be anti-symmetric with respect to $\phi_1 = \phi_0+\pi$. Then, it is easily seen that ψ^2 will be $[\phi_0+2n\pi]$–symmetric and $[\phi_0+(2n+1)\pi]$–anti-symmetric. When we compute the eigenfunction ψ^1 of H_1 by $\psi^1 = \frac{i}{\tilde{\epsilon}}\mathcal{A}^\dagger\psi^2$, this eigenfunction will change the character in ϕ_0 so that it will be $[\phi_0+2n\pi]$–anti-symmetric and $[\phi_0+(2n+1)\pi]$–anti-symmetric. From ψ^1 we can get an eigenfunction of H_2 by translation: $\tilde{\psi}^2(\phi) = \psi^1(\phi+\pi)$. In this way we get a new eigenfunction $\tilde{\psi}^2$ that has the same symmetric character as the initial ψ^2. Therefore, as they could be proportional we can not say whether they are linearly dependent or independent. In other words, the symmetry does not tell us anything about the degeneracy of the spectrum of anti-periodic eigenfunctions. An example of anti-periodic eigenfunction for $\alpha = 0$ is given in Fig. 9, where it is shown the mixed symmetric/anti-symmetric character of the components $\psi^1(\phi), \psi^2(\phi)$ around the points $\phi_n = \pm\pi/2$.

4.2 Sporadic degeneracy for $k_z \neq 0$

Besides the degeneracy for periodic solutions that applies to the case $\alpha = 0$, there is another type of degeneracy for both periodic and anti-periodic solutions, which depends on the values of the parameters $\alpha \neq 0$ and $\tilde{\epsilon}$. For instance, one can appreciate in Fig. 3 (left) that for the value $(\alpha = 4, \tilde{\epsilon} = 4.61)$ there must be a degeneracy of periodic solutions, while in Fig. 8 (left), the values $(\alpha = 1.5, \tilde{\epsilon} = 2.23)$, $(\alpha = 2.5, \tilde{\epsilon} = 3.6)$, $(\alpha = 3.5, \tilde{\epsilon} = 5)$ will correspond to degenerate anti-periodic solutions. As this new type of degeneracy will be present only for some specific pair of values of $(\alpha, \tilde{\epsilon})$, it will be called 'sporadic'.

The origin of the sporadic degeneracy relies in the symmetry relation $V_1(-\phi) = V_2(\phi)$, as can be seen in Fig. 2. The procedure to characterize the sporadic degeneracy values $(\alpha, \tilde{\epsilon})$ consists in the following steps.

a) Find a symmetric or anti-symmetric solution ψ^2 of H_2 for an specific pair of values $(\alpha, \tilde{\epsilon})$ (if it does exist!).

b) By means of the operator $\mathcal{A}^+$, following the relation (15), construct the associate solution ψ^1 of H_1. Since $W(\phi)$, given in (23), has no symmetry for $\alpha \neq 0$, the solution ψ^1 will not be symmetric nor anti-symmetric.

c) As $H_1(-\phi) = H_2(\phi)$, a second solution $\tilde{\psi}^2$ of H_2 will be given by $\tilde{\psi}^2(\phi) = \psi^1(-\phi)$. Then, $\tilde{\psi}^2$ and ψ^2 must be linearly independent since the initial function ψ^2 is sym-

metric or anti-symmetric while $\tilde{\psi}^2$ is not. In conclusion, for such values $(\alpha, \tilde{\epsilon})$ there will be a degeneracy given by ψ^2 and $\tilde{\psi}^2$.

Therefore, according to the above procedure, in order to obtain an sporadic degeneracy, it is enough to compute particular solutions with an even/odd symmetry. Such a type of solutions can be found in a simple way for our particular magnetic field.

Consider for instance the case of anti-periodic solutions. An even anti-periodic solution is given, for example, by (we hare restricting to the case $\tilde{\epsilon}^2 > M + N$, $\alpha > 0$)

$$\psi^2(\phi) = \begin{cases} (-1)^n \frac{k_2}{k_1} \sin(k_1(\phi + \pi/2)), & -\pi < \phi < -\pi/2, \quad k_1 = 2n \\ \cos(k_2\,\phi), & -\pi/2 < \phi < \pi/2, \quad k_2 = 2n+1 \qquad n \in \mathbb{N}\,. \\ -(-1)^n \frac{k_2}{k_1} \sin(k_1(\phi - \pi/2)), & \pi/2 < \phi < \pi, \quad k_1 = 2n \end{cases} \tag{44}$$

This type of functions satisfy the matching conditions (29). According to the values of k_1 and k_2 for the solutions given in (28), they are determined by the equations

$$\begin{cases} k_1^2 = \tilde{\epsilon}^2 - (M+N) = (2n)^2 \\ k_2^2 = \tilde{\epsilon}^2 - (M-N) = (2n+1)^2\,. \end{cases} \tag{45}$$

Once fixed the integer value n and, for example, the parameters $\beta = 1, A_0 = 1$, then the two equations (45) will give us the values $(\tilde{\epsilon}, \alpha)$ of the corresponding sporadic degeneracy:

$$\text{Degenerate even solutions}: (\alpha = 2n + \frac{1}{2},\ \tilde{\epsilon}^2 = 8n^2 + 4n + 1), \quad n \in \mathbb{N}\,. \tag{46}$$

Odd anti-periodic solutions are given, for instance, by (also in the case $\tilde{\epsilon}^2 > M+N$, $\alpha > 0$)

$$\psi^2(\phi) = \begin{cases} (-1)^n \frac{k_2}{k_1} \sin(k_1(\phi + \pi/2)), & -\pi < \phi < -\pi/2, \quad k_1 = 2n-1 \\ \sin(k_2\,\phi), & -\pi/2 < \phi < \pi/2, \quad k_2 = 2n \qquad n \in \mathbb{N}\,. \\ (-1)^n \frac{k_2}{k_1} \sin(k_1(\phi - \pi/2)), & \pi/2 < \phi < \pi, \quad k_1 = 2n-1 \end{cases} \tag{47}$$

This time, once fixed n, β, A_0, the degeneracy values of $\alpha, \tilde{\epsilon}$ are given by

$$\begin{cases} k_1^2 = \tilde{\epsilon}^2 - (M+N) = (2n-1)^2 \\ k_2^2 = \tilde{\epsilon}^2 - (M-N) = (2n)^2\,. \end{cases} \tag{48}$$

Hence, in this example, for $\beta = 1, A_0 = 1$, the degeneracy values are

$$\text{Degenerate odd solutions}: (\alpha = 2n - \frac{1}{2},\ \tilde{\epsilon}^2 = 8n^2 - 4n + 1), \quad n \in \mathbb{N}\,. \tag{49}$$

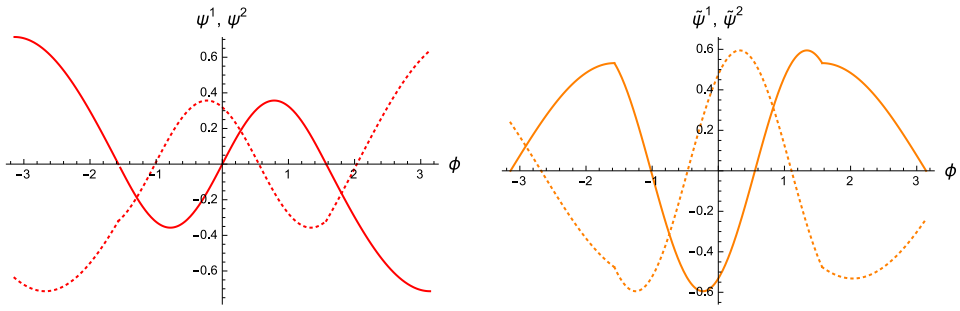

Figure 11: Anti-periodic functions of a 'sporadic' degenerate energy $\tilde{\epsilon} = \sqrt{5}$, $\alpha = 1.5, \beta = 1, A_0 = 1$. The first anti-periodic eigenfunction $\Psi = (\psi^1, \psi^2)^T$ is plotted to the left and the second $\tilde{\Psi} = (\tilde{\psi}^1, \tilde{\psi}^2)^T$ to the right. The first components $\psi^1, \tilde{\psi}^1$ are represented by dashing curves while the second ones $\psi^2, \tilde{\psi}^2$ are in continuous curves. Remark that ψ^2 is an odd anti-periodic function as mentioned in (50).

According to (46) and (49), the first values of sporadic degeneracy of anti-periodic solutions are therefore:

$$\begin{aligned} &(\alpha = 1.5,\ \tilde{\epsilon}^2 = 5), && \text{odd} \\ &(\alpha = 2.5,\ \tilde{\epsilon}^2 = 13), && \text{even} \\ &(\alpha = 3.5,\ \tilde{\epsilon}^2 = 25), && \text{odd}\,. \end{aligned} \tag{50}$$

Such values can be observed in Fig. 8 (left). The independent solutions for the first case $(\alpha = 1.5, \tilde{\epsilon}^2 = 5)$ are shown in Fig. 11.

The case of sporadic degeneracy for the periodic solutions can be studied in a similar way. Just for completeness we will supply the first sporadic periodic values for $\beta = 1, A_0 = 1$,

$$\begin{aligned} &\text{Even solutions}: (\alpha = 4n,\ \tilde{\epsilon}^2 = 20n^2 + \tfrac{5}{4}), && n = 1, 2, \ldots \\ &\text{Odd solutions}: (\alpha = 4n - 2,\ \tilde{\epsilon}^2 = 20n^2 - 20n + 6 + \tfrac{1}{4}), && n = 2, 3, \ldots \end{aligned} \tag{51}$$

The first value of degeneracy is the even solution $(\alpha = 4, \tilde{\epsilon}^2 = 21.25)$, which can be appreciated in Fig. 12 (left). Following this procedure in a straightforward way, a complete list of all the sporadic degeneracies can be given for this magnetic field.

5 Conclusions

This work has been devoted to explain the degeneracy of the energy levels in a nanotube under transverse magnetic fields in the continuous approximation of massless Dirac equation. We have considered the case of a magnetic field described by means of Dirac delta distributions. This type of magnetic field is not usual in nanotubes but it has been studied

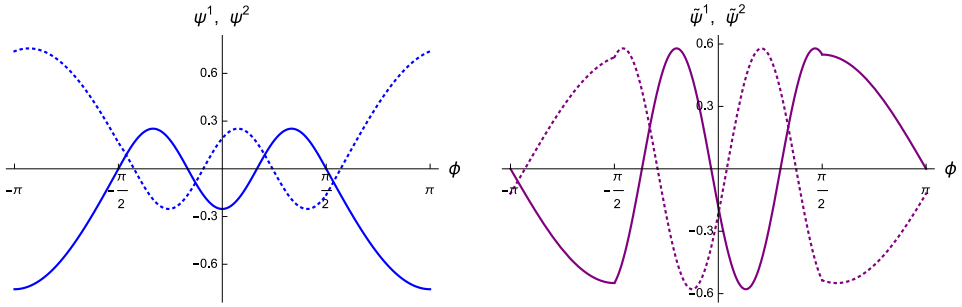

Figure 12: Periodic functions of a 'sporadic' degenerate energy $\tilde{\epsilon} = \sqrt{21.25}$, $\alpha = 4, \beta = 1, A_0 = 1$. The first anti-periodic eigenfunction $\Psi = (\psi^1, \psi^2)^T$ is plotted to the left and the second $\tilde{\Psi} = (\tilde{\psi}^1, \tilde{\psi}^2)^T$ to the right. The first components $\psi^1, \tilde{\psi}^1$ are represented by dashing curves while the second ones $\psi^2, \tilde{\psi}^2$ are in continuous curves. Remark that ψ^2 is an even periodic function as mentioned in (51).

in different configurations related to graphene [12, 13], where our considerations can be extended for the periodic cases.

The main conclusion is that there exists degeneracy for the periodic solutions corresponding to null axial momentum $k_z = 0$. This type of degeneracy is present under quite general symmetry conditions, so that it is also found, for example, in the case of a constant background magnetic field as given in [4, 7] or in elliptic potentials [11]. There can be another type of more restricted degeneracy that we call 'sporadic'. This new degeneracy is present in our example for some periodic and anti-periodic solutions, but it depends on very special conditions of the magnetic field.

The degeneracy of energy levels has important effects on the electronic properties of the nanotube. In the case of the degeneracy for $k_z = 0$ and high field intensities, it persists for the ground level even when $|k_z| > 0$ (see Fig. 3), which gives rise to an special quantum Hall effect for thick nanotubes [7]. The sporadic degeneracy is only present in higher levels, so its consequences are not so evident. However, the sporadic degeneracy leads to an increase of the density of states and it will also drastically affect to the current properties for the corresponding specific values of (E, k_z). In the case of periodic magnetic fields in graphene, where our considerations still apply, the sporadic degeneracy will suppress a forbidden band at the degenerating values of (E, k_z) giving rise to a wider allowed band.

In order to prove the different types of degeneracy we have made use of the underlying supersymmetry of the massless Dirac Hamiltonian. The supersymmetric structure of the massless Dirac Hamiltonian has already been used in some previous works to show different properties in graphene, nanotubes or fullerenes [4, 10, 11, 14, 15].

Acknowledgments

We acknowledge financial support from Spanish MINECO, project MTM2014-57129. Ş. Kuru acknowledges the warm hospitality at Department of Theoretical Physics, University of Valladolid, Spain.

References

[1] R. Saito, G. Dresselhaus and M. S. Dresselhaus, *Physical properties of carbon nanotubes* (Imperial College Press, London, 1998).

[2] J. -C. Charlier, X. Blase and S. Roche, Rev. Mod. Phys. **79**, 677 (2007) and references therein.

[3] C.L. Kane and E.J. Mele, Phys. Rev. Lett. **78**, 1932 (1997).

[4] H.-W. Lee, Dmitry S. Novikov, Phys. Rev. B **68**, 155402 (2003).

[5] H. Ajiki and T. Ando, J. Phys. Soc. Jpn. **62**, 1255 (1993).

[6] J. P. Lu, Phys. Rev. B **74**, 1123 (1995).

[7] E. Perfetto, J. González, F. Guinea, S. Bellucci and P. Onorato, Phys. Rev. B **76**, 125430 (2007).

[8] S. Bellucci, J. González, F. Guinea, P. Onorato and E. Perfetto J. Phys.: Condens. Matter **19**, 395017 (2007).

[9] N. Nemec and G. Cuniberti, Phys. Rev. B **74**, 165411 (2006).

[10] Ş. Kuru, J. Negro and L.M. Nieto, J. Phys.: Condens. Matter **21**, 455305 (2009).

[11] V. Jakubsky, Ş. Kuru and J. Negro, J. Phys. A: Math. Theor. **47**, 115307 (2014).

[12] M. Ramezani Masir, P. Vasilopoulos and F.M. Peeters, New J. Phys. **11**, 095009 (2009).

[13] S. Ghosh and M. Sharma, J. Phys.: Condens. Matter **21**, 292204 (2009).

[14] V. Jakubsky, Ş. Kuru, J. Negro and S. Tristao, J. Phys.: Condens. Matter **25**, 165301 (2013).

[15] B. Midya, D.J. Fernández, J. Phys. A: Math. Theor. **47**, 285302 (2014).